Computational Studies of Liquid Water and Diluted Water in Carbon Tetrachloride

Tsun-Mei Chang

Department of Chemistry, University of Wisconsin−Parkside, 900 Wood Road, Box 2000, Kenosha, Wisconsin 53141

Liem X. Dang*

Chemical and Materials Sciences Division, Pacific Northwest National Laboratory, Richland, Washington 93352

Received: November 21, 2007; In Final Form: January 7, 2008

Molecular dynamics simulations were carried out to study solvent effects on the energetic and dynamical properties of water molecules in liquid water and in carbon tetrachloride (CCl_4). In these studies, the free-energy profiles or potentials of mean force (PMF) for water dimers in both solvents were computed. The computed PMF results showed a stable minimum near 3 Å for the O−O separation, with a minimum free energy of about −2.8 kcal/mol in CCl_4, as compared to a value of −0.5 kcal/mol in liquid water. The difference in free energy in water as compared to that in CCl_4 was expected and is the result of competition from surrounding water molecules that are capable of forming hydrogen bonds in the liquid water. This capability is absent in the diluted water found in CCl_4. We found that the rotational motions of H_2O/D_2O were nonisotropic, with the out-of-plane vector correlation times in H_2O/D_2O varying from 5.6/5.8 ps at 250 K to 0.57/0.56 ps at 350 K and the corresponding OH/OD bond vectors varying from 6.5/7.7 ps to 0.75/0.75 ps. The results compare reasonably well to the available NMR experimental and computer simulation data on the same system (Farrar; Skinner; et al. *J. Am. Chem. Soc.* **2001**, *123*, 8047). For diluted water in CCl_4, we found the computed rotational correlation times also were nonisotropic and much longer than the corresponding NMR experimental values at the same concentration (Farrar; et al. *J. Phys. Chem.* A **2007**, *111*, 6146). Upon analyzing the water hydrogen-bonding patterns as a function of water concentration, we conclude that the differences in the rotational correlation times mainly result from the formation of water hydrogen-bonding networks as the water concentration is increased in liquid CCl_4. In addition, we found the rotational correlation times to be substantially faster in liquid CCl_4 than in liquid water.

I. Introduction

The structure, energetics, and dynamics of water molecules in various environments play an important role in many chemical, biological, and environmental processes. A molecular-level understanding of how the water−solvent interactions that govern the dynamical properties of water is essential to understanding their characteristics. Significant progress has been made in advancing the understanding of water dynamics as a function of temperature and water concentration in nonaqueous solutions and liquid water. Early contributions included the work of Farrar and Skinner and their co-workers on the rotational motion in liquid water.[1] In addition to obtaining good agreement between experimental and theoretical results, their results also indicated that the rotational motion of water is anisotropic (i.e., the in-plane and out-of-plane rotation times are different). Farrar and co-works recently reported an additional study on the rotational motion of a dilute solution (0.03 mol %) of water in CCl_4.[2] This study concluded that the water dynamics in CCl_4 is anisotropic and significantly faster than that in liquid water, mainly because water molecules rotate freely due to the limited probability of forming hydrogen-bonding networks with their partners in CCl_4.

In this paper, we report a series of molecular dynamics (MD) simulations to examine the solvation properties of water molecules in aqueous solution and in CCl_4. To the best of our knowledge, this work differs from early MD contributions in the methodology (i.e., potential model and constrained mean force technique) and the properties of which we intend to calculate. In addition to calculating the dynamical properties of water molecules in both solvents, we also study the solvent effects on the dimerization of water in liquid water and in CCl_4. By comparing the computed PMFs for water dimers in both solvents, we are able to demonstrate the influence of hydrogen bonding on the interactions of water dimers in aqueous systems. We also demonstrate in these MD studies of water/D_2O molecules in bulk water and in CCl_4 that because of strong hydrogen-bonding interactions between water molecules, the rotational motion of water/D_2O in bulk is highly hindered and rotates quite slowly. On the other hand, a much faster rotational motion of water is expected because of weak interactions between water/D_2O and CCl_4. This behavior has been observed in recent nuclear magnetic resonance (NMR) experiments.[2] Quantitatively, we found that the computed rotational correlation times from the simulations at the experimental conditions (i.e., 0.03 mol %) yielded values significantly larger than those resulting from experimental efforts. Upon analyzing the factors that may explain this observation, we concluded that the differences in the rotational correlation times mainly result from the formation of water hydrogen-bonding networks as the additional water molecules are added to the liquid CCl_4.

* Corresponding author. E-mail: liem.dang@pnl.gov.

10.1021/jp711092v CCC: $40.75
Published on Web 01/31/2008

We note here that our simulation differs from most previous studies on water dynamics by explicitly including the polarizabilities for both solvents and solute molecules. This approach allowed us to probe the interactions at finer level of detail. Other simulation studies have contributed to our understanding of the rotational dynamics of liquid water at room temperature.[3−6] In section II of this paper, we briefly describe the computational details of the molecular dynamics simulations. In section III, the potentials of mean force between two water molecules in bulk and in CCl_4 are examined. The structure and the dynamical properties of water/D_2O in water and CCl_4 are also discussed in section III. Our conclusions are presented in section IV.

II. Potential Models and Computational Methods

Details of the molecular models, including the determination of the induced dipole from polarizabilities, are given in our previous published work.[7,8] The incorporation of polarization effects explicitly into potential models provides insight into the adaptability of the monomer dipole moment in clusters and of interfacial environments. The averaged water dipole moment of the diluted water in carbon tetrachloride (CCl_4) will have a different value when it is compared to the liquid water because of the difference in the electric field. In addition, the potential of mean force (PMF) of the water dimer in CCl_4 will have a different well-depth when the polarizability is excluded from the potential model. The PMFs and dynamical calculations were carried out using a modified version of AMBER v7.0.[9] We employed the constrained mean force technique to calculate the PMFs.[10,11] The following expressions were used to calculate the solute−solute mean force as an average over the different configurations:

$$F(r) = \frac{1}{2}\langle \mathbf{r}_u(\mathbf{F}_A - \mathbf{F}_B)\rangle \tag{1}$$

In this expression, $\mathbf{r}_u$ is a unit vector along the AB direction and is defined as

$$\mathbf{r}_u = (r_A - r_B)/|r_A - r_B| \tag{2}$$

$\mathbf{F}_A$ and $\mathbf{F}_B$ are the forces acting on the solutes A and B, respectively, and the angular brackets indicate the ensemble average. The PMF, $W(r)$ is calculated as

$$W(r) = -\int_{r_0}^{r_s} F_r \, dr \tag{3}$$

Here, r_0 and r_s are the initial and final separation distances between the water dimer center of mass. The computed PMF was anchored so that it is zero at $r = r_s$. The center-of-mass distance between the water dimer in 548 water molecules or in 398 CCl_4 molecules was incremented in 0.20 Å increments. At each center-of-mass separation the average **F**(r) was determined from 350 ps of simulation time, preceded by 100 ps of equilibration. The uncertainties were ±0.1 kcal/mol as estimated by determining the force averaged over four equally spaced time frames during the production.

We calculate translational dynamics and rotational correlation times from the corresponding autocorrelation functions. The translation motion of the water molecules (water/D_2O) in liquid water and in CCl_4 is described by the velocity autocorrelation function:

$$C(t) = \frac{\langle \vec{V}(t)\cdot\vec{V}(0)\rangle}{\langle \vec{V}(0)\cdot\vec{V}(0)\rangle} \tag{4}$$

TABLE 1: Simulation Details[a]

x_W	0.005	0.01	0.02	0.03
N_{water}	2	4	8	12
N_{CCl_4}	398	396	392	388

[a] x_W is the mole fraction of water in the liquid phase. N_{water} and N_{CCl_4} are the numbers of water and CCl_4 molecules used in the simulations.

where $V(t)$ and $V(0)$ are the center-of-mass velocities of water molecules at time t and time 0, respectively. The corresponding spectral density is defined as

$$f(w) = \int_0^\infty e^{-iwt} C(t)\, dt \tag{5}$$

The rotational dynamics and the corresponding correlation times of water molecules in liquid water and in CCl_4 can be examined via the following descriptions:

$$C_2(t) = \langle P_2[\hat{u}(0)\cdot\hat{u}(t)]\rangle \tag{6}$$

and

$$\tau = \int_0^\infty C_2(t)\, dt \tag{7}$$

where $\hat{u}(t)$ is the body-fixed unit vector along the principal axis of the molecular coordinate system at time t and $P_2(x)$ denotes the second Legendre Polynomial. In the water molecule, the principal axis is the OH/OD bond vector, and the out-of-plane motion is the vector that corresponds to motion of orthogonal unit vectors.

The MD simulations were performed on pure water and several water−CCl_4 mixtures with the water mole fraction, x_W, ranging from 0.005 to 0.03. The number of water and CCl_4 molecules used in the simulations is listed in Table 1. The linear dimension of the cubic simulation system is roughly equal to 40 Å. During the entire simulation, periodic boundary conditions were applied in all three directions. The systems were first equilibrated in a constant pressure-temperature (NPT) ensemble. The temperature of the system was maintained at 298 K by coupling the water and CCl_4 to external thermal baths with a time constant of 2 ps via the Berendsen scheme.[12] The velocities generated from a Maxwell−Boltzmann distribution at 298 K were assigned to each atom initially. All bond lengths in the system were constrained by the SHAKE algorithm.[13] A time step of 2 fs was used to integrate the equations of motion. A nonbonded interaction cutoff of 11 Å was employed, and the smooth particle mesh Ewald method was used to account for the long-range Coulombic and polarization interactions. After an initial equilibration for 500 ps in an NPT ensemble, the subsequent MD simulations were performed in an NVE ensemble with a 1 fs time step. A 700 ps trajectory was carried out to equilibrate the system, followed by 1 ns period of data collection for analysis. Similar MD simulations were performed for D_2O in D_2O and in CCl_4. We simply replaced the mass of the H atom with that of a D atom, while keeping all the other potential parameters constant.

III. Results and Discussion

A. Potentials of Mean Force of Water Dimer. We begin by discussing the results of the computed PMFs in liquid water and in CCl_4. In Figure 1, we present the computed PMFs using the constrained mean force technique as described in the previous section for the water dimer in liquid water and in CCl_4 as a function of the water dimer center-of-mass separation. According to statistical mechanics, the free energy, $W(r)$, is also

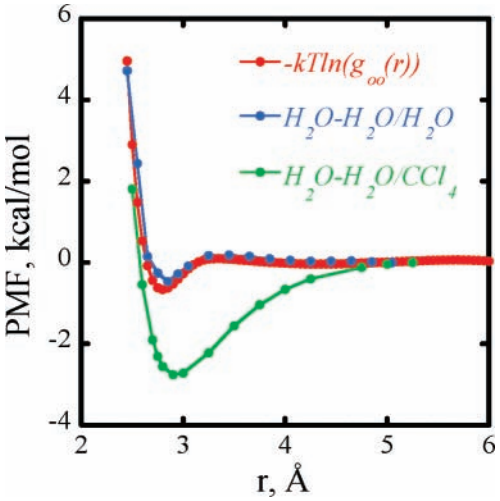

Figure 1. Computed PMFs for water dimer in liquid water and CCl_4.

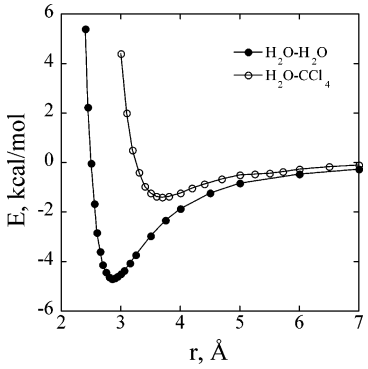

Figure 2. Potential energies for water dimer and water−CCl_4.

related to the radial distribution functions, $g(r)$, as described by the following relationship:

$$W(r) = -k_b T \ln(g_{oo}(r)) \tag{8}$$

Here, k_b is the Boltzmann's constant. The computed free-energy profile from the O−O radial distribution function in liquid water is also depicted in Figure 1. Clearly, there is an excellent agreement between the free-energy curves obtained from the PMF calculations and that of the radial distribution function, indicating that PMF calculations provide a reliable method for evaluating free-energy profiles. Upon analyzing Figure 1, we can summarize our findings as follows. First, although their characteristics are not unexpected, the details of the PMF results provide interesting insights into the molecular interactions. We observed significant differences in these PMFs; in particular, the free-energy minimum for the water dimer in liquid water is significantly smaller than the corresponding value in CCl_4 (i.e., −0.5 compared to −2.8 kcal/mol). Second, we can reason this difference in terms of the dimer energies as shown in Figure 2. Because the computed water dimer energy is almost three times the size of the water−CCl_4 dimer energy, one might expect the hydrogen-bonding configuration of the water dimer remains intact for a wide range of separation in CCl_4, until the water−CCl_4 interaction overtakes the water−water interaction. In other words, it is easier to dimerize the water molecules in CCl_4 than in liquid water. Third, we note that there is a small free-energy barrier (i.e., 0.5 kcal/mol) begins around 3.25 Å in the free-energy profile of the water dimer in bulk, which is probably due to the water dimer contacting with the solvent molecules as its separation become larger. There had been a study of solvent contribution to the PMFs of water dimer in liquid water by Mezei and Ben-Naim,[14] but unfortunately, the water dimer orientations were fixed in their simulations, and the water−water interaction energy was not included in the computed PMFs. Therefore, a quantitative comparison to their reported results is not feasible.

B. Translational and Rotational Dynamics in Liquid Water. To understand the structural and dynamical properties of water molecules in different solvent environments, we analyzed the velocity autocorrelation functions, the orientational autocorrelation functions, and the hydrogen-bonding distribution of water molecules in bulk and in the hydrophobic CCl_4 solvent as a function of the water mole fraction. By comparing the results of these analyses, we gained insight into how hydrogen bonding affects the rotational motion of water molecules.

We begin this discussion with the low-frequency end of the spectral density in the region from 0 to 300 cm^{-1}. This region can, in part, be examined by the spectral intensity of the motion of molecular center-of-mass. In Figure 3, the computed translational velocity autocorrelation function (VACF) of the water center-of-mass and the corresponding spectral density at room temperature is shown. The temperature dependence of the translational dynamics is also shown in Figure 3. We observe prominent variations in the center-of-mass motion as a function of temperature. The oscillation strength (i.e., the intensity) is noticeably larger at 250 K when compared to the intensity found at 350 K. In all cases, we found that the spectral densities of the center-of-mass motion have two peaks, one at ∼60 cm^{-1} and another at ∼200 cm^{-1} (see the insets in Figure 3). The pronounced band at 200 cm^{-1} has been tentatively identified as the O−O intermolecular stretching motion, and the broad band centered around 50 cm^{-1} has been accounted for as the three body O−O−O bending motion.[15−17] We note here that our results are similar to those reported in other studies on the same system.[3−6] We also calculated the translational diffusion coefficients of the water center-of-mass by integrating over the velocity autocorrelation function. We found that the diffusion coefficient increased as the temperature increased, ranging from 0.2×10^{-5} to 6.0×10^{-5} cm^2/s betweem 250 and 350 K. Similar results and observations obtained for translational dynamics of D_2O water molecules are graphically depicted in Figure 4.

The rotational correlation functions, $C_2(t)$, as a function of time for the OH/OD bond vectors at room temperature are plotted in Figures 5 and 6. Clearly, these correlation functions cannot be described by single-exponential decays. They exhibit a rather rapid initial decay on the order of 0.025 ps, followed by a much slower decay that seems to be well approximated by a single-exponential function. These correlation functions exhibit similar characteristics as those obtained in the simulation study by Skinner and co-workers[1] using a different water potential model. We also found that the decay in the correlation functions is much more rapid at higher temperatures (data not shown), indicating a faster rotational motion. The out-of-plane correlation functions behave in a manner similar to those of the OH/OD bond vector—a fast initial decay followed by a slower decay (data not shown). We computed the water/D_2O rotational correlation times for both vectors and compared these results with the corresponding experimental data. Agreement with the observed data is quite good at 300 K and above. Our results and the corresponding experimental data for the rotational times of the out-of-plane vector are depicted in Figure 7.

C. Translational and Rotational Dynamics of the Dilute Water in CCl_4. Because of the weak interactions between water/D_2O and CCl_4 molecules, one may expect that the translational

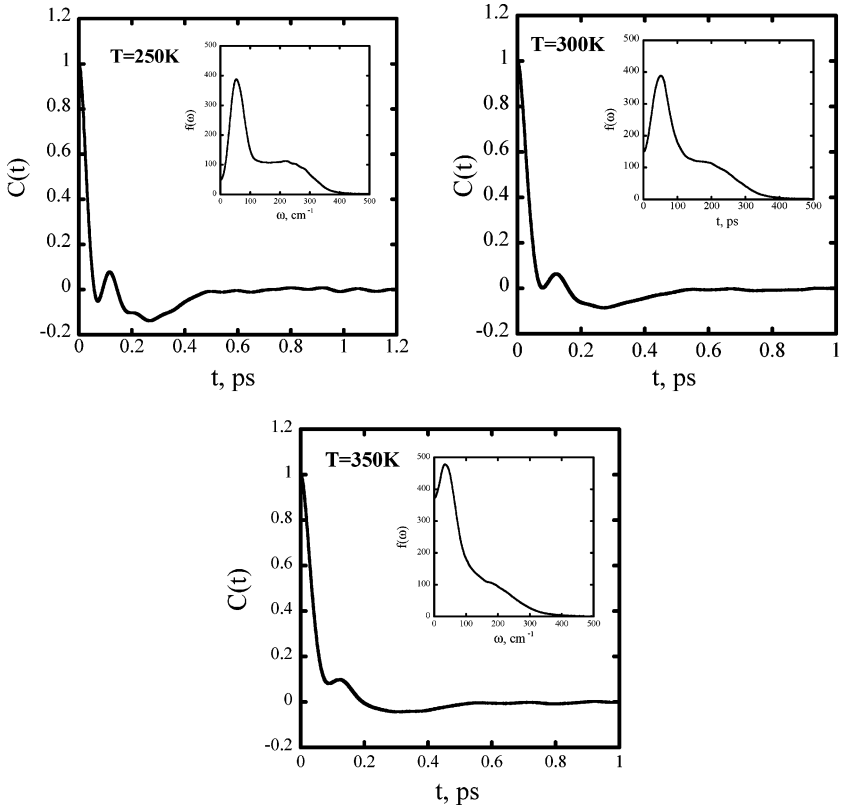

Figure 3. Translational velocity autocorrelations and the corresponding spectral densities for liquid water at 250, 300, and 350 K.

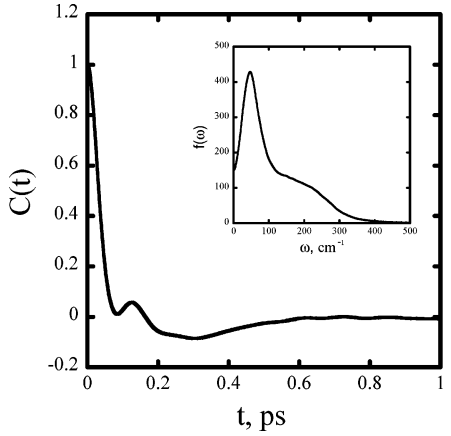

Figure 4. Translational velocity autocorrelation and the corresponding spectral density for liquid water (D_2O) at 300 K.

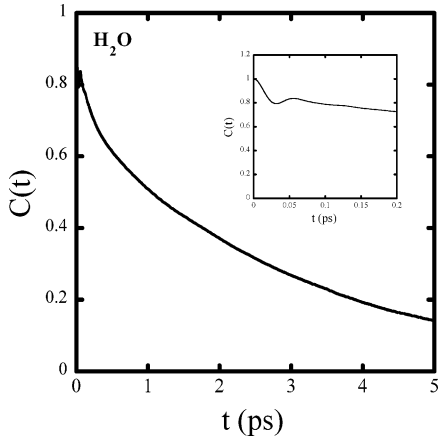

Figure 5. Rotational autocorrelation function for the OH bond vector of liquid water (H_2O) in bulk at 300 K.

motion of water/D_2O in CCl_4 is stochastic and diffusive. In Figure 8, the normalized velocity autocorrelation function at room temperature of the water in CCl_4, $C(t)$, is shown as a function of time at two water mole fractions, $x_W = 0.005$ and 0.03. Both velocity autocorrelation functions show an initial decay to zero in about 0.2 ps. However, there are subtle differences between these two curves. The VACF at $x_W = 0.005$ seems to be well approximated by a simple decay followed by a minor oscillation around zero. The negative portion of the autocorrelation function before it decays to zero suggests the motion of the water may be slightly hindered at short times. On the other hand, the VACF of water at $x_W = 0.03$ displays a more complicated behavior. At the shorter time scale, the translational motion of water displays a fast decay up to 0.1 ps. At about 0.1 ps, the diffusion becomes hindered and decays with a slower rate as indicated by the changing slope in VACF. This behavior may be related to the high probability of hydrogen-bond formation at the higher concentrations, which will be discussed later in this paper. As a result, the estimated diffusion constants are 6.3×10^{-5} and 4.0×10^{-5} cm^2/s for water in CCl_4 at $x_W = 0.005$ and 0.03, respectively. These values are faster than the self-diffusion constant of water in bulk. This trend can be understood on the basis of the weaker interactions between water and CCl_4; hence, the water can move more freely. As the water concentration increases, the increasing probability of forming hydrogen bonds with other water molecules causes a slowdown of the diffusive motions of water molecules.

An alternative method for obtaining the diffusion constant is to use the mean-square displacements based on the Einstein relation[18]

$$D = \frac{1}{6} \lim_{t \to \infty} \frac{d}{dt} \langle |\vec{r}(t) - \vec{r}(0)|^2 \rangle \qquad (9)$$

where $\vec{r}(t)$ are the center-of-mass coordinates of the water at time t. The mean-square displacement of water from MD

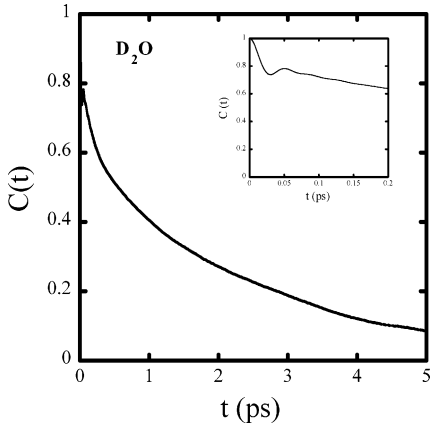

Figure 6. Rotational autocorrelation function for the OD bond vector of liquid water (D_2O) in bulk at 300 K.

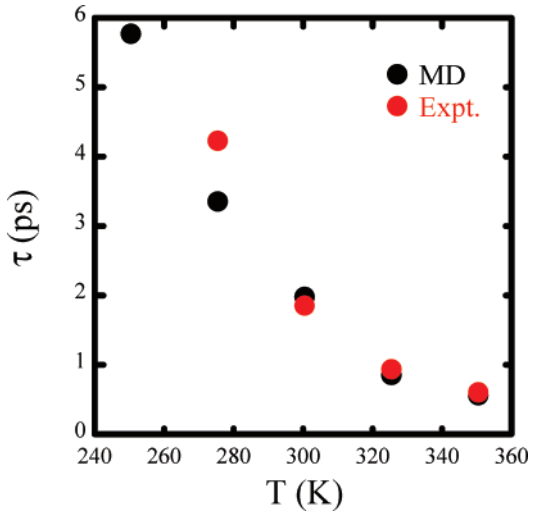

Figure 7. Comparison of the calculated rotational times of the water out-of-plane vector with the corresponding experimental measurements for liquid water (D_2O) at 300 K.

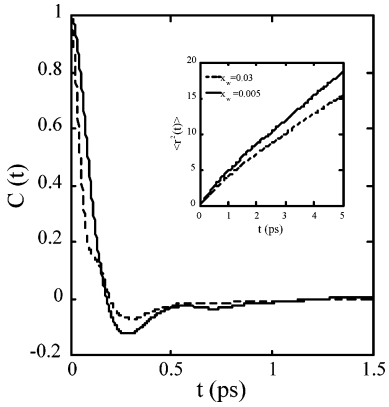

Figure 8. Normalized velocity autocorrelation functions at 300 K of the dilute water in CCl_4. Insets are the corresponding mean squared displacements.

simulations at 298 K is plotted as a function of time as the inset in Figure 8. It is clear that water diffuses more quickly in the more dilute solutions. The diffusion constants were estimated from the least-square fits to be 5.5×10^{-5} and 3.5×10^{-5} cm^2/s for $x_W = 0.005$ and 0.03 solution, respectively, which are in reasonable agreement with the VACF analysis.

The rotational motion of water in dilute CCl_4 solution can be examined via the rotational autocorrelation function, $C_2(t)$. The water principal axes are chosen to be O−H bond vector

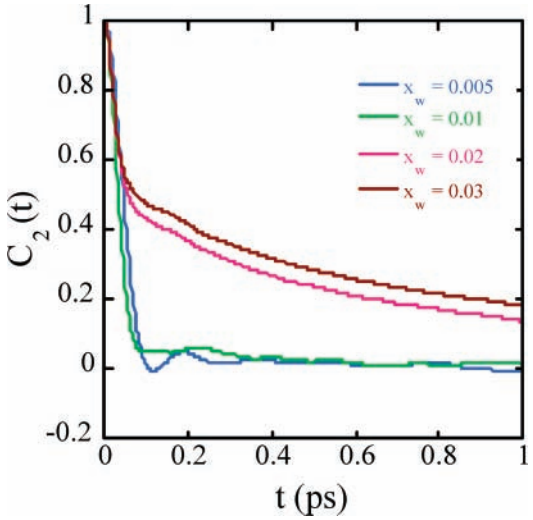

Figure 9. Normalized rotational autocorrelation function at room temperature for the OH bond vector of the dilute water in CCl_4 at various concentrations.

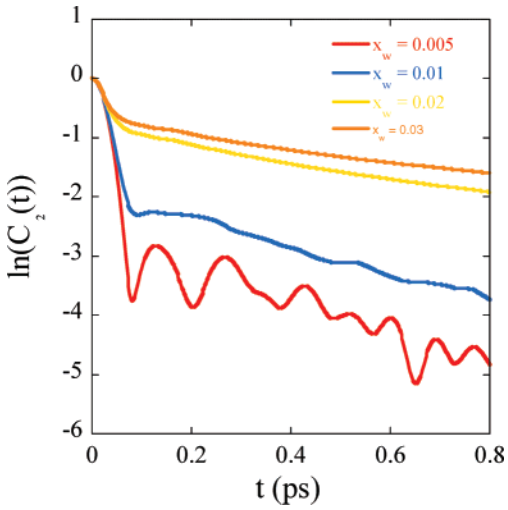

Figure 10. $\ln(C_2(t))$ of the rotational autocorrelation function of H_2O in CCl_4.

and the out-of-plane vector to enable comparison with the results available from NMR experiments. The rotational correlation functions as a function of time for the OH bond vector are plotted in Figure 9. The different curves correspond to various water concentrations. Clearly, these correlation functions cannot be described by single-exponential decays. They exhibit very rapid decay initially, followed by much slower decays that can be approximated by a single-exponential function. This trend can be more easily recognized by plotting the $\ln(C_2(t))$ as a function of time as is shown in Figure 10. One clearly sees that there are roughly two regimes for the rotational motion of water molecules in CCl_4. At short time scale up to 0.1 ps, the rotational autocorrelation functions decay quickly at distinct rates that decrease as the water concentration increases. This behavior seems to imply an inverse correlation between the initial rotational motion and the probability of forming hydrogen bonds with other water molecules. When water molecules begin to rotate, the interactions between the water and the surrounding molecules will be altered; hence, the initial rates may reflect the local bonding environments of water molecules. At the higher water mole fraction, the probability of water being hydrogen-bonded is enhanced significantly. The rotation of water may destroy the favorable directional hydrogen-bonding

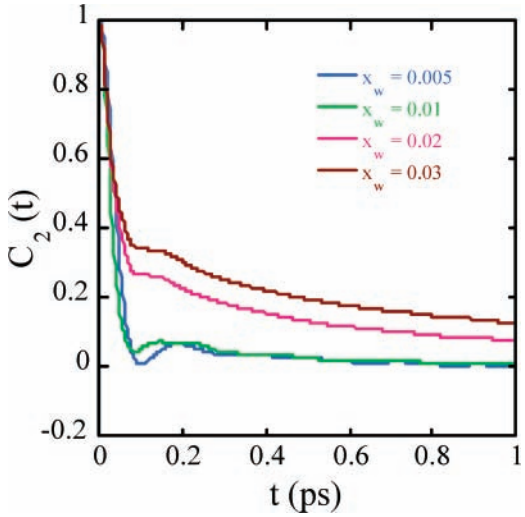

Figure 11. Normalized rotational autocorrelation function at room temperature of the out-of-plane vector for dilute water (H_2O) in CCl_4 at various concentrations.

TABLE 2: Rotational Correlation Times for Water (H_2O/D_2O) in CCl_4 Solutions

	τ_{OH} (fs)	τ_O (fs)	τ_{OD} (fs)	τ_O (fs)
$x_W = 0.005$	55.7	64.1	74.7	71.8
$x_W = 0.01$	109	83.0	116	89.4
$x_W = 0.02$	393	256	462	308
$x_W = 0.03$	545	389	642	445

interaction, leading to highly hindered rotational motion. On the other hand, the rotation of water in an environment composed mostly of CCl_4 molecules will not experience such an impediment and will rotate quite freely. After the initial decay, all correlation functions exhibit a slower decay with similar rates, which would be expected on the basis of the long-time diffusive rotational behavior of the water molecules.

In Figure 11, the rotational correlation functions for the out-of-plane vector of water are shown as a function of time for the dilute water/CCl_4 solutions. In general, the out-of-plane correlation functions behave in a manner similar to those of the OH bond vector—a fast initial decay followed by a slower decay. The most noticeable difference is that the correlation functions of the out-of-plane vector seem to show a much faster initial decay especially at higher water concentrations. This indicates that the rotational motion of water may be anisotropic.

The rotational correlation times– of the OH bond vectors (τ_{OH}) and of the out-of-plane (τ_O) can be obtained by integrating the rotational correlation functions. These data are summarized in Table 2. One clearly sees that except at the lowest concentration, τ_{OH} and τ_O have distinct values, which supports our conclusion that the rotational motion is anisotropic. Both rotational correlation times are observed to increase significantly with increasing water concentration, which may result from the formation of water hydrogen-bonding networks as the water concentrations increase in liquid CCl_4 as was discussed earlier.

We also examined the rotational motion of D_2O in CCl_4 and found that the rotational correlation functions of D_2O decay slightly slower than those of water in CCl_4. The rotational correlation times are found to increase considerably and become anisotropic as the water concentration is increased in CCl_4. These results are compared to the recent NMR experimental data reported by Farrar and co-workers[1,2] on the same D_2O/CCl_4 systems. They also obtained different rotational correlation times and found that the rotational motion is anisotropic. However, our simulations yield much longer correlation times

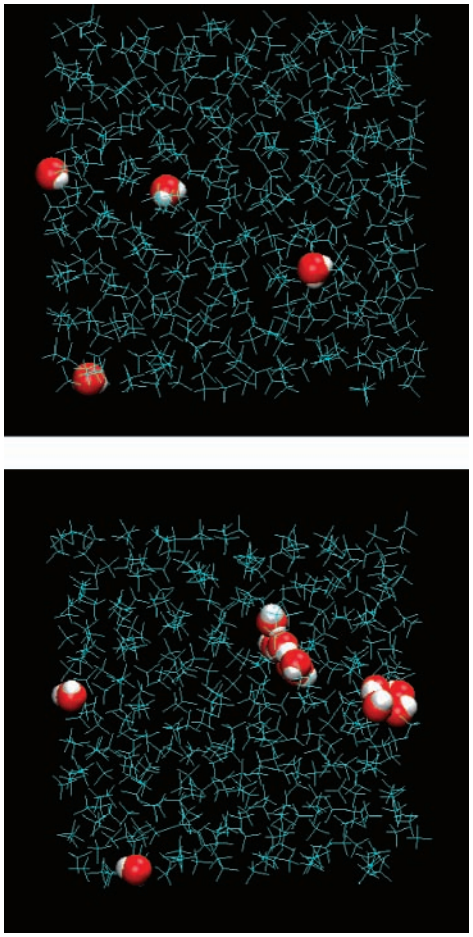

Figure 12. Snapshots taken from MD simulations of 0.01 and 0.03 mol % of D_2O in CCl_4.

than their results at the same concentration. Interestingly, at a lower concentration, our calculated results agree reasonably well with the experimental values. The difference may come from the enhanced probability of forming a hydrogen-bonding network in our simulations as demonstrated in Figure 12, which are snapshots taken from 0.01 and 0.03 mol % solutions of MD simulations. One can see clearly that the water clusters are formed in the 0.03 mol % solution but not in the 0.01 mol % simulation. It will also be interesting in the future to investigate how the system size affects the hydrogen-bonding patterns in the simulations

D. Hydrogen-Bonding Distribution. In our MD simulations, we examined the probability that water molecules form hydrogen bonds with each other in CCl_4 as a function of its mole fraction, x_W. Two water molecules are considered hydrogen-bonded when their O···O separation is less than 3.5 A, the O···H distance is less than 2.6 A, and the angle between OH bond and H···O vector is greater than 127°. We employed these hydrogen-bonding criterion using our configurationally water dimer minimum energy. Others have used slightly different hydrogen-bonding criterion in their studies. Additionally, we also analyzed the size distribution of the hydrogen-bonding networks. Note that the largest size of the cluster is restricted by the number of water molecules in the systems. It would be interesting to see how the distribution changes by varying the system size. However, in this study, we are mainly interested in solvent effects on the water dynamics, so we will leave that question for future studies.

In Table 3, the probability of water molecule participating in a hydrogen-bonded cluster of size n is listed. Clearly, as the

TABLE 3: Size Probability Distribution of the Water Hydrogen-Bonding Network as a Function of the Mole Fraction of Water, X_W

cluster size, n	$x_W = 0.005$	$x_W = 0.01$	$x_W = 0.02$	$x_W = 0.03$
1	0.99351	0.7610	0.5694	0.5743
2	0.00649	0.1972	0.0441	0.0916
3		0.0417	0.0031	0.0041
4			0.0058	0.0006
5			0.0433	0.0006
6			0.2391	0.0015
7			0.0271	0.0068
8			0.0681	0.0245
9				0.1125
10				0.1067
11				0.0769
12				0.0000
in cluster	0.00649	0.23897	0.43058	0.42573

mole fraction of water increases, the probability of finding water in hydrogen-bonded clusters increases. At the lowest mole fraction of $x_W = 0.005$, the majority of the water molecules are free, spending less than 1% of the time associating with each other. At higher concentrations, a significant amount of water molecules (up to 40%) are found to participate in hydrogen bonding. This result is not surprising because there are more water molecules available for hydrogen bonding at higher concentrations. It is also observed that once the water molecule participated in hydrogen bonding, it persisted for quite some time before it dissociated. The relative stability of the hydrogen bonding is supported by the minimum in the free-energy profile observed in the PMF calculation as was discussed in the previous section. A similar trend also was observed for D_2O in CCl_4.

As discussed previously, the rotational correlation times of water (and D_2O) in CCl_4 solution increases as the water mole fraction increases. This trend can be correlated with the formation of hydrogen-bonding clusters. When a water molecule is in the network of hydrogen bonds, the rotation will distort the favorable directional hydrogen bonding and incur an energy penalty. As a direct consequence, the rotation motion is highly hindered and leads to a much slower rotation in the more concentrated solutions. This finding demonstrates that solvent−solute interactions play an important role in determining the dynamical properties of water in solutions.

IV. Conclusions

We carried out MD simulations to study solvent effects on the energetic and dynamical properties of water molecules in liquid water and in CCl_4. In these studies, we found the free-energy profiles or PMFs of water dimers in both solvents are significantly different from each other. The computed PMF results showed a stable minimum near 3 Å for the O−O separation with a minimum free energy of about −2.8 kcal/mol in CCl_4, as compared to a value of −0.5 kcal/mol determined for liquid water. The difference in free energies mainly results from competition between water molecules (hydrogen bonding) in liquid water, which does not occur in the diluted water in CCl_4. We found the rotational motions are nonisotropic, with the out-of-plane vector correlation times in H_2O/D_2O varying from 5.6/5.8 ps at 250 K to 0.57/0.56 ps at 350 K and the corresponding OH/OD bond vectors varying from 6.5/7.7 ps to 0.75/0.75 ps. Our results are in reasonable agreement with the results available from NMR experiments and other computer simulations on the same system. For the diluted water in CCl_4, we found that the computed rotational correlation times also are nonisotropic and much longer than indicated by corresponding data from NMR experimental studies at the same concentration. We analyzed the water hydrogen-bonding patterns as a function of water concentrations and concluded that the differences in the rotational correlation times mainly result from the formation of water hydrogen-bonding networks as the water concentration increases in liquid CCl_4. Furthermore, the observed clustering in the simulation at 0.03 mol % solution may be an artifact of the small system sizes. We can validate this point by performing additional simulations with larger system sizes. We found the rotational correlation times are substantially faster in liquid CCl_4 than in the bulk water.

Acknowledgment. This work was supported by the Office of Basic Energy Sciences of the U.S. Department of Energy, in part by the Chemical Sciences Program and in part by the Engineering and Geosciences Division. The Pacific Northwest National Laboratory is operated by Battelle for the DOE.

References and Notes

(1) Ropp, J.; Lawrence, C.; Farrar, T. C.; Skinner, J. L. *J. Am. Chem. Soc.* **2001**, *123*, 8047.
(2) Goodnough, J. A.; Goodrich, L.; Farrar, T. C. *J. Phys. Chem. A* **2007**, *111*, 6146.
(3) Kuo, I. F. W.; Mundy, C. J.; Eggimann, B. L.; McGrath, M. J.; Siepmann, J. I.; Chen, B.; Vieceli, J.; Tobias, D. J. *J. Phys. Chem. B* **2006**, *110* (8), 3738.
(4) Chowduri, S.; Tan, M. L.; Ichiye, T. *J. Chem. Phys.* **2006**, *125*, 144513.
(5) Harder, E.; Eaves, J. D.; Tokmakoff, A.; Berne, B. J. *Proc. Nat.l Acad. Sci.* **2005**, *102* (33), 11611.
(6) Lefohn, A. E.; Ovchinnikov, M.; Voth, G. A. *J. Phys. Chem. B* **2001**, *105*, 6628.
(7) Dang, L. X.; Chang, T. M. *J. Chem. Phys.* **1997**, *106*, 8149.
(8) Chang, T. M.; Petersen, K. A.; Dang, L. X. *J. Chem. Phys.* **1995**, *103*, 7052.
(9) Case, D. A.; Pearlman, D. A.; Caldwell, J. W.; et al. AMBER 7, 7th ed.; University of California: San Francisco, 2002.
(10) Ciccotti, G.; Ferrario, M.; Hynes, J. T.; Karpal, R. *Chem. Phys.* **1989**, *129*, 241.
(11) Guardia, E.; Rey, R.; Padro, J. A. *Chem. Phys.* **1991**, *155*, 187.
(12) Berendsen, H. J. C.; Postma, J. P. M.; Vangunsteren, W. F.; Dinola, A.; Haak, J. R. *J. Chem. Phys.* **1984**, *81*, 3684.
(13) Ryckaert, J.-P.; Ciccotti, G.; Berendsen, H. J. C. *J. Comput. Phys.* **1977**, *23*, 327.
(14) Mezei, M.; Ben-Naim, A. *J. Chem. Phys.* **1990**, *92*, 1359.
(15) Sceats, M. G.; Rice, S. A. *J. Chem. Phys.* **1980**, *72*, 3236.
(16) Madden, P. A.; Imprey, R. W. *Chem. Phys. Lett.* **1985**, *123*, 503.
(17) Bopp, P.; Dietz, W.; Heizinger, K. *Z. Naturforsch* **1979**, *34a*, 1424.
(18) Allen, M. P.; Tidesley, D. J. *Computer Simulation of Liquids*; Clarendon Press: Oxford, U.K., 1987.